

---

**ELECTRODYNAMICS  
AND WAVE PROPAGATION**

---

## Method of Integral Equations for the Solution of Diffraction Problems about the Calculation of Twisted Guiding Structures

S. M. Garanin<sup>a, \*</sup>, I. N. Danilov<sup>a</sup>, S. B. Raevskii<sup>b</sup>, and A. Yu. Sedakov<sup>a</sup>

<sup>a</sup>*Sedakov Scientific-Research Institute of Measuring Systems, Nizhny Novgorod, 603950 Russia*

<sup>b</sup>*Alekseev Nizhny Novgorod State Technical University, Nizhny Novgorod, 603950 Russia*

\**e-mail: garanin\_s.m@mail.ru*

Received December 20, 2018; revised December 20, 2018; accepted January 11, 2019

**Abstract**—The method of integral equations is suggested for calculating irregular twisted guided structures. The method is based on the Lorentz integral relationship and makes it possible to solve internal diffraction problems for waveguides, whose screening surface is described by analytical functions.

**DOI:** 10.1134/S1064226920020060

### INTRODUCTION

This work is devoted to the description of the numerical–analytical method for calculating the transmission characteristics of a twisted waveguide having a rectangular cross-section. This method is a variant of the method of integral equations, which is formulated in works [1, 2] on the basis of the integral form of the Lorentz lemma. The ideology of the method is stated in work [3] for the first time.

The waveguide twisted joint is an irregular section of a screened waveguiding structure having a rectangular cross-section. In this structure, only the position of the cross-section contour changes depending on the longitudinal coordinate rather than its shape and dimensions. The contour position is determined by angle  $\Phi(z)$  of its rotation with respect to the similar contour of the twisted joint beginning. This angle depends on longitudinal coordinate  $z$ . Irregular sections of a microwave section that have the type of a twisted joint are most often applied in antenna devices [4] for the rotation of a polarization plane.

The problem of diffraction by a waveguide twisted joint can be solved using such widespread and electro-dynamically justified methods as the method of cross-sections [5, 6] and the partial domain method (PDM) [7, 8]. The first method is used for calculating the transmission characteristics of irregular guiding structures having parameters that slowly change along the longitudinal coordinate [5]. Therefore, its application for calculating waveguide twisted joints that are short with respect to the longitudinal coordinate and have a respectively large value of the rotation angle of the polarization plane (of compact twisted joints) leads to obtaining results with a considerable error. The second method (PDM) can be applied to calculating

twisted joints with arbitrary values of lengths and rotation angles of the polarization plane. However, this method calls for large expenses of the computer time and a cumbersome procedure of the algebraization of a calculating algorithm.

The numerical–analytical method suggested in this work for calculating the transmission characteristics of longitudinally–azimuthally irregular waveguiding structures has advantages over the methods indicated above both in the counting rate and in the sufficiently simple procedure of the problem algebraization.

### 1. THE METHOD OF INTEGRAL EQUATIONS IN THE DIFFRACTION PROBLEM ABOUT THE TRANSMISSION CHARACTERISTICS OF A WAVEGUIDE TWISTED JOINT HAVING A RECTANGULAR CROSS- SECTION

The considered guiding section is schematically shown in Fig. 1. It is volume  $V$  bounded by the surfaces  $S = S_1 + S_2 + S_3$  and  $S_{1,2}$ .

In this volume, electromagnetic fields  $(\vec{E}_1; \vec{H}_1)$  and  $(\vec{E}_2; \vec{H}_2)$  created by sources  $\vec{j}_1^{e,m}$  and  $\vec{j}_2^{e,m}$ , respectively, exist. Here,  $S_1$  and  $S_3$  are the side surfaces of the first (region I) and second (region III) regular waveguides, respectively;  $S_2$  is the side surface of the irregular region of the waveguide twisted joint (region II) with length  $L$  along longitudinal coordinate  $z$ ; and  $S_{1,2}$  are the cross-section planes bounding the region of the considered guiding structure along longitudinal coordinate  $z$ .

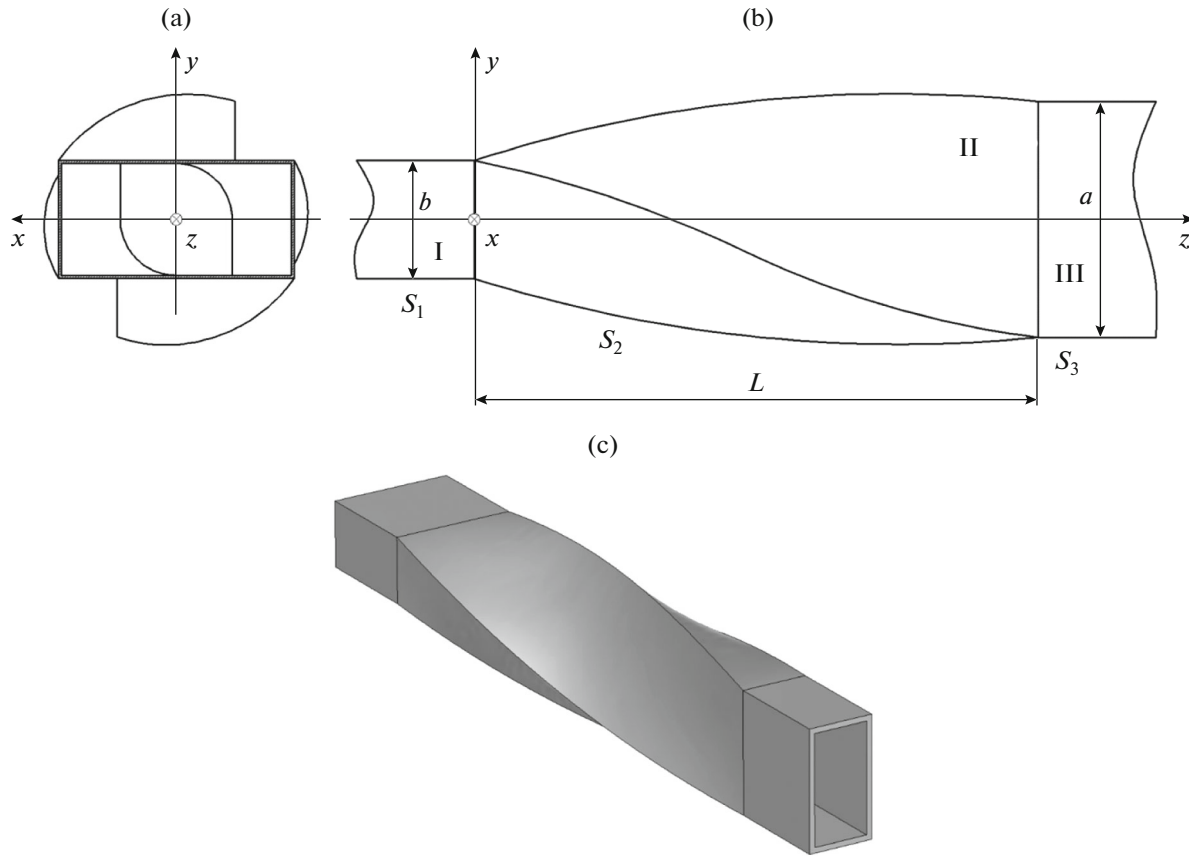


**Fig. 1.** Waveguide twisted joint connecting coaxial regular rectangle screened waveguides rotated with respect to each other by the angle of 90° around the z axis: (a) front view, (b) lateral view, and (c) overall view.

The indicated fields and sources are connected by the following relationship according to the Lorentz lemma:

$$\oint_{S+S_{1,2}} ([\vec{E}_1, \vec{H}_2] - [\vec{E}_2, \vec{H}_1]) \cdot d\vec{S} = \int_V (\vec{j}_1^e, \vec{E}_2 - \vec{j}_2^e, \vec{E}_1 - \vec{j}_1^m, \vec{H}_2 + \vec{j}_2^m, \vec{H}_1) dV. \tag{1}$$

As fields  $\vec{E}_1$  and  $\vec{H}_1$  we use the solutions to the Maxwell equations that correspond to the wave propagating in the guiding structure and on surface  $S$  satisfy the boundary conditions of the continuity of the electric field tangential component and magnetic field normal component

$$E_\tau|_S = 0, \quad H_n|_S = 0. \tag{2}$$

Sources  $\vec{j}_2^{e,m}$  are auxiliary, and they are situated in the finite region inside the guiding structure near the surface  $z = 0$ . These sources create the spherical wave field satisfying the zero boundary condition at the points situated infinitely far from the sources. The specificity of the formulation of the Lorentz lemma in this case is in the fact that the lemma is written for the fields corresponding to different boundary value problems in one and the same volume. One boundary value

problem is formulated for the irregular waveguide, and the second one is formulated for the unbounded space. This formulation of the Lorentz lemma can be called generalized.

According to the technique suggested in work [1], we infinitely remove sections  $S_{1,2}$  from the coordinate origin ( $z_{1,2} \rightarrow \pm\infty$ ) and take into account that sources  $\vec{j}_1^{e,m}$  moved at  $z_{1,2}$  create in the open space spherical wave field  $(\vec{E}_0; \vec{H}_0)$  that satisfies the conditions

$$|\vec{E}_0(\vec{r}_{j_2^{e,m}})| \ll |\vec{E}_1(\vec{r}_{j_2^{e,m}})|, \quad |\vec{H}_0(\vec{r}_{j_2^{e,m}})| \ll |\vec{H}_1(\vec{r}_{j_2^{e,m}})|$$

at the place, where the auxiliary sources are located.

Then, we can exclude currents  $\vec{j}_1^{e,m}$  from Eq. (1) and, choosing elementary electric and magnetic dipoles as auxiliary sources, obtain the Fredholm integral equations of the second kind

$$\int_S ([\vec{H}_1, \vec{E}_2], d\vec{S}) = -I_0^e L E_1(\vec{r}_{j_2^e}), \tag{3}$$

$$\int_S ([\vec{H}_1, \vec{E}_2], d\vec{S}) = I_0^m L H_1(\vec{r}_{j_2^m}). \tag{4}$$

Solving integral equations (3) and (4) and using boundary conditions (2), we determine desired fields

$\vec{E}_1$  and  $\vec{H}_1$  in the irregular guiding structure. At the same time, there are no limitations of the waveguide twisted joint length measured along the longitudinal coordinate and of the value characterizing the rotation angle of the transverse section contour of the second regular waveguide relative to the same contour of the first waveguide.

Consider the guiding structure schematically shown in Fig. 1. The transverse dimensions of the first (region I) and second (region III) waveguides as well as of the region of the waveguide twisted joint (region II) are identical. The dimension of the cross-section wide wall is  $a$ , and the dimension of the narrow wall is  $b$ . Let one of the eigenmodes of the first waveguide be incident from the side of this waveguide. As the result of this wave diffraction taking place in the irregular region of the waveguide twisted joint, an infinite set of reflected waves is excited in the first waveguide. The reflection coefficients are  $R_{mn}^E$  for the  $E$  waves and  $R_{mn}^H$  for the  $H$  waves. An infinite set of transmitted waves is formed in the second waveguide. The transmission coefficients are  $B_{mn}^E$  for the  $E$  waves and  $B_{mn}^H$  for the  $H$  waves.

The longitudinal components of the electric and magnetic fields in region I ( $-\infty < z \leq 0$ ) are written as follows:

$$E_{zI}(x, y, z) = \left(\chi_{mn}^{(I)}\right)^2 \sin\left(\frac{\pi m}{a}\left(x + \frac{a}{2}\right)\right) \times \sin\left(\frac{\pi n}{b}\left(y + \frac{b}{2}\right)\right) \exp(-j\beta_{mn}^{(I)}z) + \sum_{m,n=0}^{\infty} R_{mn}^E \left(\chi_{mn}^{(I)}\right)^2 \sin\left(\frac{\pi m}{a}\left(x + \frac{a}{2}\right)\right) \times \sin\left(\frac{\pi n}{b}\left(y + \frac{b}{2}\right)\right) \exp(j\beta_{mn}^{(I)}z), \quad (5)$$

$$H_{zI}(x, y, z) = \left(\chi_{mn}^{(I)}\right)^2 \cos\left(\frac{\pi m}{a}\left(x + \frac{a}{2}\right)\right) \times \cos\left(\frac{\pi n}{b}\left(y + \frac{b}{2}\right)\right) \exp(-j\beta_{mn}^{(I)}z) + \sum_{m,n=0}^{\infty} R_{mn}^H \left(\chi_{mn}^{(I)}\right)^2 \cos\left(\frac{\pi m}{a}\left(x + \frac{a}{2}\right)\right) \times \cos\left(\frac{\pi n}{b}\left(y + \frac{b}{2}\right)\right) \exp(j\beta_{mn}^{(I)}z), \quad (6)$$

where  $\chi_{mn}^{(I)}$  is the transverse wave number of rectangular waveguide I and  $\beta_{mn}^{(I)}$  is the longitudinal wave number of rectangular waveguide I.

The remaining components of the electric and magnetic fields of the electromagnetic waves are expressed (see, for example, [9]) from the Maxwell equations using components (5) and (6)

$$\text{curl } \vec{H} = j\omega\varepsilon\vec{E}, \quad \text{curl } \vec{E} = -j\omega\mu\vec{H}, \quad (7)$$

where  $\varepsilon$  and  $\mu$  are the medium permittivity and permeability, respectively.

We obtain the expressions for the transverse components of field intensities of the electric type waves from Eqs. (7)

$$E_x = \frac{1}{\chi_{mn}^2} \frac{\partial^2 E_z}{\partial x \partial z}, \quad H_x = \frac{j\omega\varepsilon}{\chi_{mn}^2} \frac{\partial E_z}{\partial y}, \quad (8)$$

$$E_y = \frac{1}{\chi_{mn}^2} \frac{\partial^2 E_z}{\partial y \partial z}, \quad H_y = -\frac{j\omega\varepsilon}{\chi_{mn}^2} \frac{\partial E_z}{\partial x}.$$

The transverse components of the fields of the magnetic type waves are expressed in terms of the longitudinal components as

$$E_x = -\frac{j\omega\mu}{\chi_{mn}^2} \frac{\partial H_z}{\partial y}, \quad H_x = \frac{1}{\chi_{mn}^2} \frac{\partial^2 H_z}{\partial x \partial z}, \quad (9)$$

$$E_y = \frac{j\omega\mu}{\chi_{mn}^2} \frac{\partial H_z}{\partial x}, \quad H_y = \frac{1}{\chi_{mn}^2} \frac{\partial^2 H_z}{\partial y \partial z}.$$

All the components of the electromagnetic fields of the  $H$ - and  $E$ -type waves in waveguide I can be written using relationships (5), (6), (8), and (9).

The connection of wave numbers in region I ( $-\infty < z \leq 0$ ) looks as follows:

$$\varepsilon\mu\omega^2 = \left(\chi_{mn}^{(I)}\right)^2 + \left(\beta_{mn}^{(I)}\right)^2. \quad (10)$$

The transverse wave numbers in region I are determined as

$$\chi_{mn}^{(I)} = \sqrt{\left(\frac{\pi m}{a}\right)^2 + \left(\frac{\pi n}{b}\right)^2}. \quad (11)$$

Since the transverse dimensions of regions I, II, and III remain invariant, relationships (10) and (11) are valid for the whole considered guiding structure

$$\chi_{mn}^{(I)} = \chi_{mn}^{(II)} = \chi_{mn}^{(III)} = \chi_{mn}, \quad \beta_{mn}^{(I)} = \beta_{mn}^{(II)} = \beta_{mn}^{(III)} = \beta_{mn}.$$

For the solution of the considered diffraction problem it is necessary to have the expressions for the field components of the  $E$ - and  $H$ -type waves on the surface of the irregular region and on the surface of the second regular screened rectangular waveguide. An auxiliary regular comparison waveguide (CW) [5] is matched with each transverse section of the considered guiding structure in order to write the field components on the surface and find the values of the surface integrals over the irregular region of this structure. The CW has the same section and distribution of the filling medium parameters. The desired field is sought in the form of the superposition of the CW proper wave fields. The fields on the CW end boundaries are joined indirectly using integral equations (3) and (4) [2] rather than in the explicit form using the boundary conditions. The amplitude coefficients of electromagnetic waves are determined as solutions of an inhomogeneous system of linear algebraic equations (SLAEs).

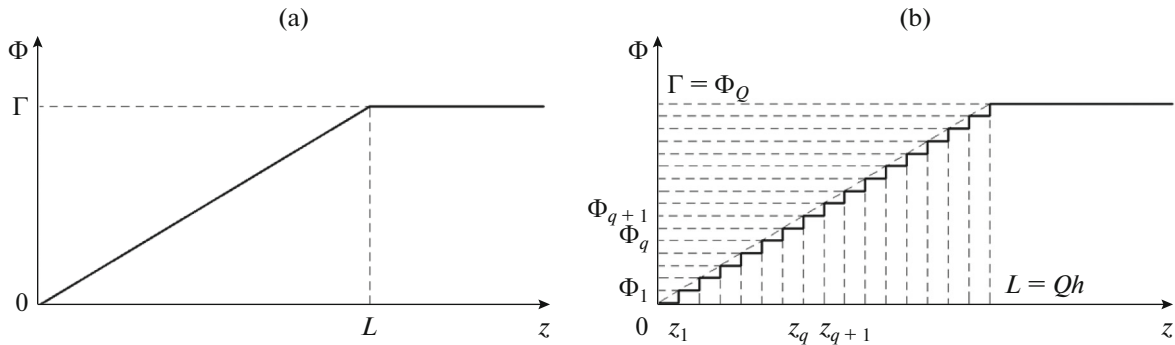


**Fig. 2.** Dependence of the rotation angle of the polarization plane of the waveguide twisted joint on the  $z$  coordinate: (a)  $\Phi(z)$  dependence and (b) stepwise approximation of the  $\Phi(z)$  dependence.

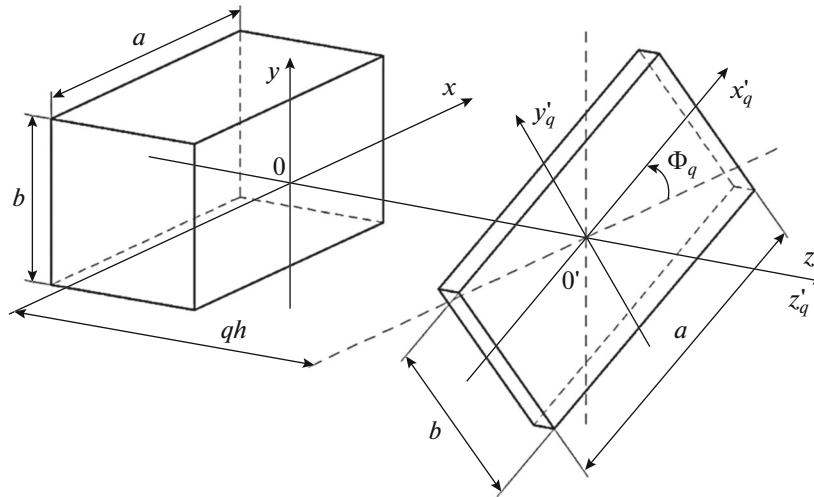


**Fig. 3.** Relative orientation of the BCS and  $LCS_q$  in the investigated waveguide structure.

Thus, we practically succeed in representing the irregular region of the twisted joint as the cascade connection of finite number  $Q$  of guiding structure sections in the form of regular CWs having dimension  $h$  along longitudinal coordinate  $z$ . The dimensions of the wide and narrow walls in the transverse section of each such waveguide are  $a$  and  $b$ , respectively. We call Cartesian system  $(x, y, z)$  the base coordinate system (BCS). Every CW having the dimensions  $a \times b \times h$  is turned around BCS axis  $z$  through angle  $\Phi = \Phi(z)$  depending on the value of longitudinal coordinate  $z$ . Figure 2a shows dependence  $\Phi(z)$  in irregular region II ( $0 < z < L$ ) and in the region of the second regular waveguide ( $L \leq z < \infty$ ). Figure 2b shows the stepwise approximation of the linear dependence of  $\Phi(z)$ . This approximation corresponds to the representation of the irregular region in the form of the cascade of CWs. Index  $q$  in the figure corresponds to the ordinal number of a regular CW,  $Q$  is the number of the indicated CWs in the twisted joint, and  $h$  is the dimension of the step of the twisted joint discretization. The CW length along the longitudinal coordinate is  $z$ . Angle  $\Gamma$  is the rotation angle of the contour of the transverse section of the second regular waveguide with respect to the

same contour of the first waveguide. When  $z \geq L$ , this angle does not depend on longitudinal coordinate  $z$ . Therefore, in Figs. 2a and 2b, dependence  $\Phi(z)$  for  $z \geq L$  is a straight line parallel to axis  $z$ .

Figure 3 shows the mutual orientation of the first regular waveguide and the  $q$ th CW. The Cartesian coordinate system  $(x'_q, y'_q, z'_q)$  shown in the figure is called the local coordinate system (LCS) of the  $q$ th CW. Below, it is called the  $LCS_q$ . This system is inflexibly connected with the surface of the  $q$ th CW. Namely, the two  $LCS_q$  axes (the axes  $x'_q$  and  $y'_q$ ) lie in the CW transverse section as it is shown in the figure. The direction of the  $z'_q$  axis coincides with the vector of the phase velocity (coinciding with the  $z$  axis) of the electromagnetic wave propagating in the waveguide twisted joint. It is seen from the figure that  $LCS_q$   $(x'_q, y'_q, z'_q)$  in the irregular region rotates with respect to BCS  $(x, y, z)$  around the  $z$  axis through the same angle as the contour of the considered transverse section in the region of the twisted joint.

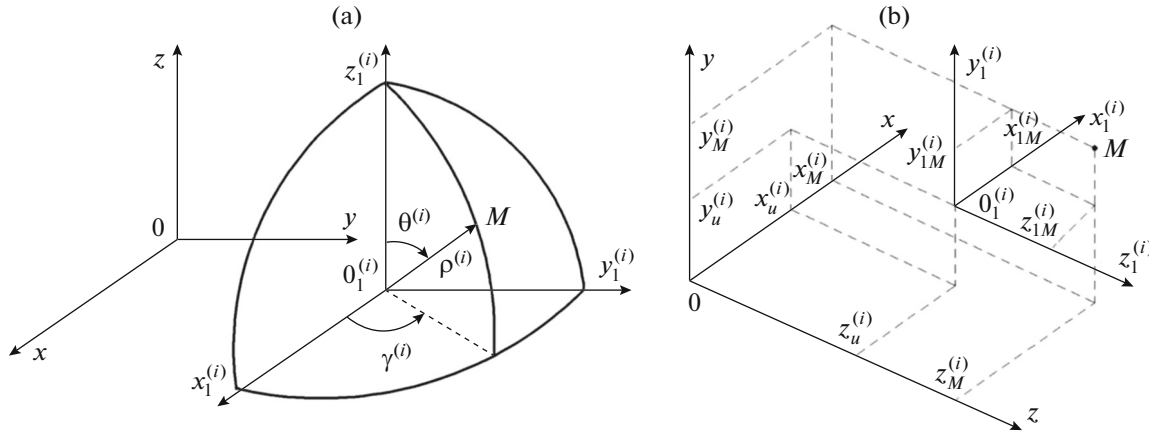


**Fig. 4.** Relative orientation: (a) of the BCS and spherical coordinate system, in which the field of the auxiliary source is described, and (b) of the BCS and auxiliary coordinate system  $(x_1^{(i)}, y_1^{(i)}, z_1^{(i)})$ .

To determine the connection between the BCS and  $LCS_q$ , it is necessary to use the coordinate transformation formulas that have the form [10]

$$\begin{aligned} x'_q &= x \cos(\Phi_q) + y \sin(\Phi_q), \\ y'_q &= -x \sin(\Phi_q) + y \cos(\Phi_q), \\ z'_q &= z - qh. \end{aligned} \quad (12)$$

Using relationships (5), (6), (8), (9), and (12), we can write all the field components of the  $H$ - and  $E$ -type waves in the irregular region of the waveguide twisted joint. We obtain the expressions of the components of the electromagnetic wave fields in the region of the second regular waveguide by replacing  $\Phi_q$  by  $\Gamma$  in formula (12) and using the indicated relationships.

The fields of auxiliary sources are present in initial integral equations (3) and (4). The elementary electric and magnetic dipoles, which are longitudinally oriented, are chosen as these sources. The components of the electromagnetic field created by the magnetic dipole are represented in the following form in the spherical coordinate system:

$$\begin{aligned} E_\gamma^{m,(i)} &= \frac{jkI_0^m L}{4\pi} \sin(\theta^{(i)}) \frac{\exp(-jk\rho^{(i)})}{\rho^{(i)}} \left(1 + \frac{1}{jk\rho^{(i)}}\right), \\ H_\rho^{m,(i)} &= \frac{I_0^m L}{2\pi j\omega\mu} \cos(\theta^{(i)}) \\ &\times \exp(-jk\rho^{(i)}) \left(\frac{1}{(\rho^{(i)})^3} + \frac{jk}{(\rho^{(i)})^2}\right), \\ H_\theta^{m,(i)} &= \frac{I_0^m L}{4\pi j\omega\mu} \sin(\theta^{(i)}) \exp(-jk\rho^{(i)}) \\ &\times \left(\frac{1}{(\rho^{(i)})^3} + \frac{jk}{(\rho^{(i)})^2} - \frac{k^2}{\rho^{(i)}}\right). \end{aligned}$$

The components of the field created by the electric dipole can be represented in the form

$$\begin{aligned} H_\gamma^{e,(i)} &= \frac{jkI_0^e L}{4\pi} \sin(\theta^{(i)}) \frac{\exp(-jk\rho^{(i)})}{\rho^{(i)}} \left(1 + \frac{1}{jk\rho^{(i)}}\right), \\ E_\rho^{e,(i)} &= \frac{I_0^e L}{2\pi j\omega\epsilon} \cos(\theta^{(i)}) \exp(-jk\rho^{(i)}) \left(\frac{1}{(\rho^{(i)})^3} + \frac{jk}{(\rho^{(i)})^2}\right), \\ E_\theta^{e,(i)} &= \frac{I_0^e L}{4\pi j\omega\epsilon} \sin(\theta^{(i)}) \exp(-jk\rho^{(i)}) \\ &\times \left(\frac{1}{(\rho^{(i)})^3} + \frac{jk}{(\rho^{(i)})^2} - \frac{k^2}{\rho^{(i)}}\right). \end{aligned}$$

Here,  $k = \omega\sqrt{\mu\epsilon}$  and  $i$  is the auxiliary source number [9]. Formulas connecting spherical coordinate system  $(\rho^{(i)}, \theta^{(i)}, \gamma^{(i)})$ , in which the components of the auxiliary source fields are described, and BCS  $(x, y, z)$ , in which the components of the fields of the considered guiding structure (Fig. 4a and Fig. 4b) are written, have the form

$$\begin{aligned} \rho^{(i)} &= \sqrt{(x_1^{(i)})^2 + (y_1^{(i)})^2 + (z_1^{(i)})^2} \\ &= \sqrt{(x - x_u^{(i)})^2 + (y - y_u^{(i)})^2 + (z - z_u^{(i)})^2}, \\ \theta^{(i)} &= \arctan \frac{\sqrt{(x_1^{(i)})^2 + (y_1^{(i)})^2}}{z_1^{(i)}} \\ &= \arctan \frac{\sqrt{(x - x_u^{(i)})^2 + (y - y_u^{(i)})^2}}{(z - z_u^{(i)})}, \\ \gamma^{(i)} &= \arctan \frac{y_1^{(i)}}{x_1^{(i)}} = \arctan \frac{(y - y_u^{(i)})}{(x - x_u^{(i)})}. \end{aligned}$$

When the auxiliary sources are situated along the longitudinal direction, the components of the fields created by them have the following form in Cartesian coordinate system  $(x, y, z)$  [11]:

$$\begin{aligned}
 E_x^{m(i)} &= -E_\gamma^{m(i)} \sin(\gamma^{(i)}), \\
 E_x^{e(i)} &= E_\rho^{e(i)} \sin(\theta^{(i)}) \cos(\gamma^{(i)}) \\
 &+ E_\theta^{e(i)} \cos(\theta^{(i)}) \cos(\gamma^{(i)}), \\
 E_y^{m(i)} &= E_\gamma^{m(i)} \cos(\gamma^{(i)}), \\
 E_y^{e(i)} &= E_\rho^{e(i)} \sin(\theta^{(i)}) \sin(\gamma^{(i)}) \\
 &+ E_\theta^{e(i)} \sin(\gamma^{(i)}) \cos(\theta^{(i)}), \\
 E_z^{m(i)} &= 0, \quad E_z^{e(i)} = E_\rho^{e(i)} \cos(\theta^{(i)}) - E_\theta^{e(i)} \sin(\theta^{(i)}), \\
 H_x^{m(i)} &= H_\rho^{m(i)} \sin(\theta^{(i)}) \cos(\gamma^{(i)}) \\
 &+ H_\theta^{m(i)} \cos(\theta^{(i)}) \cos(\gamma^{(i)}), \\
 H_x^{e(i)} &= -H_\gamma^{e(i)} \sin(\gamma^{(i)}), \\
 H_y^{m(i)} &= H_\rho^{m(i)} \sin(\theta^{(i)}) \sin(\gamma^{(i)}) \\
 &+ H_\theta^{m(i)} \cos(\theta^{(i)}) \sin(\gamma^{(i)}),
 \end{aligned}$$

$$H_y^{e(i)} = H_\gamma^{e(i)} \cos(\gamma^{(i)}),$$

$$H_z^{m(i)} = H_\rho^{m(i)} \cos(\theta^{(i)}) - H_\theta^{m(i)} \sin(\theta^{(i)}), \quad H_z^{e(i)} = 0.$$

The left-hand side of Eq. (4), in which the auxiliary field created by the magnetic dipole is present, is written in the form

$$\begin{aligned}
 &\int_S \left( [\bar{H}_1, \bar{E}_2^m], d\bar{S} \right) \\
 &= \int_{S_1} \left( [(\bar{H}_1^{E(I)} + \bar{H}_1^{H(I)}), \bar{E}_2^m], d\bar{S} \right) \Big|_{-\infty < z \leq 0} \\
 &+ \int_{S_2} \left( [(\bar{H}_1^{E(II)} + \bar{H}_1^{H(II)}), \bar{E}_2^m], d\bar{S} \right) \Big|_{0 < z < L} \\
 &+ \int_{S_3} \left( [(\bar{H}_1^{E(III)} + \bar{H}_1^{H(III)}), \bar{E}_2^m], d\bar{S} \right) \Big|_{L \leq z < \infty},
 \end{aligned}$$

where  $S_1$  is the side surface of regular region I ( $-\infty < z \leq 0$ ),  $S_2$  is the side surface of irregular region II ( $0 < z < L$ ), and  $S_3$  is the side surface of regular region III ( $L \leq z < \infty$ ).

The right-hand side of this equation has the form

$$\begin{aligned}
 I_0^m L H_1(\vec{r}_{j_2}^m) &= I_0^m L (\chi_{mn})^2 \cos\left(\frac{\pi m}{a} \left(x_u^{(i)} + \frac{a}{2}\right)\right) \cos\left(\frac{\pi n}{b} \left(y_u^{(i)} + \frac{b}{2}\right)\right) \exp(-j\beta_{mn} z_u^{(i)}) \\
 &+ I_0^m L \sum_{m,n=0}^{\infty} R_{mn}^H (\chi_{mn})^2 \cos\left(\frac{\pi m}{a} \left(x_u^{(i)} + \frac{a}{2}\right)\right) \cos\left(\frac{\pi n}{b} \left(y_u^{(i)} + \frac{b}{2}\right)\right) \exp(j\beta_{mn} z_u^{(i)}) \\
 &+ I_0^m L \sum_{m,n=0}^{\infty} B_{mn}^H (\chi_{mn})^2 \cos\left(\frac{\pi m}{a} \left(x_u^{(i)} \cos(\Gamma) + y_u^{(i)} \sin(\Gamma) + \frac{a}{2}\right)\right) \\
 &\times \cos\left(\frac{\pi n}{b} \left(-x_u^{(i)} \sin(\Gamma) + y_u^{(i)} \cos(\Gamma) + \frac{b}{2}\right)\right) \exp(-j\beta_{mn} z_u^{(i)}).
 \end{aligned}$$

The left-hand side of Eq. (3), in which the auxiliary field created by the electric dipole is present, is written in the form

$$\begin{aligned}
 &\int_S \left( [\bar{H}_1, \bar{E}_2^e], d\bar{S} \right) = \int_{S_1} \left( [(\bar{H}_1^{E(I)} + \bar{H}_1^{H(I)}), \bar{E}_2^e], d\bar{S} \right) \Big|_{-\infty < z \leq 0} \\
 &+ \int_{S_2} \left( [(\bar{H}_1^{E(II)} + \bar{H}_1^{H(II)}), \bar{E}_2^e], d\bar{S} \right) \Big|_{0 < z < L} + \int_{S_3} \left( [(\bar{H}_1^{E(III)} + \bar{H}_1^{H(III)}), \bar{E}_2^e], d\bar{S} \right) \Big|_{L \leq z < \infty}.
 \end{aligned}$$

The right-hand side of Eq. (3) has the form

$$\begin{aligned}
 -I_0^e L E_1(\vec{r}_{j_2}^e) &= -I_0^e L (\chi_{mn})^2 \sin\left(\frac{\pi m}{a} \left(x_u^{(i)} + \frac{a}{2}\right)\right) \sin\left(\frac{\pi n}{b} \left(y_u^{(i)} + \frac{b}{2}\right)\right) \exp(-j\beta_{mn} z_u^{(i)}) \\
 &- I_0^e L \sum_{m,n=0}^{\infty} R_{mn}^E (\chi_{mn})^2 \sin\left(\frac{\pi m}{a} \left(x_u^{(i)} + \frac{a}{2}\right)\right) \sin\left(\frac{\pi n}{b} \left(y_u^{(i)} + \frac{b}{2}\right)\right) \exp(j\beta_{mn} z_u^{(i)}) \\
 &- I_0^e L \sum_{m,n=0}^{\infty} B_{mn}^E (\chi_{mn})^2 \sin\left(\frac{\pi m}{a} \left(x_u^{(i)} \cos(\Gamma) + y_u^{(i)} \sin(\Gamma) + \frac{a}{2}\right)\right) \\
 &\times \sin\left(\frac{\pi n}{b} \left(-x_u^{(i)} \sin(\Gamma) + y_u^{(i)} \cos(\Gamma) + \frac{b}{2}\right)\right) \exp(-j\beta_{mn} z_u^{(i)}).
 \end{aligned}$$

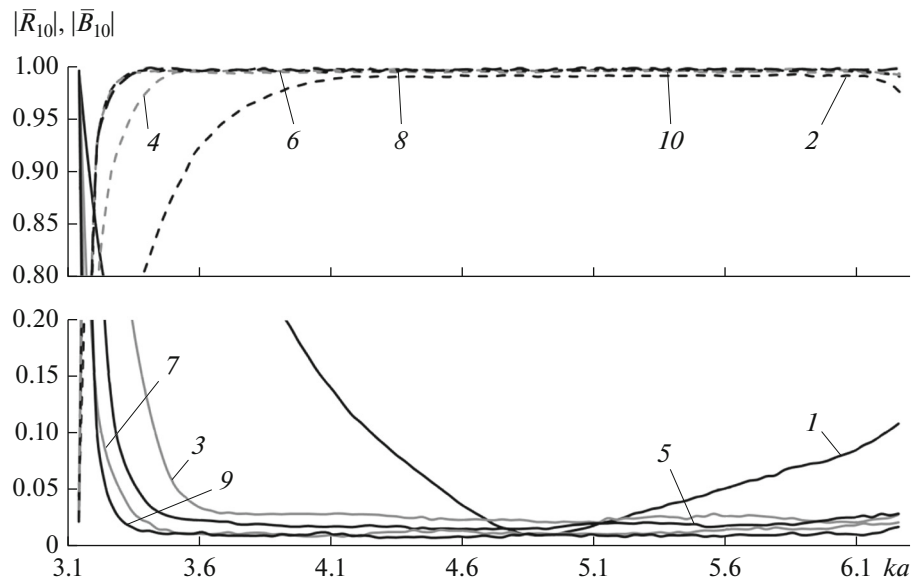


**Fig. 5.** Dependences of the absolute values of the (solid lines) reflection ( $|\bar{R}_{10}|$ ) and (dashed lines) transmission ( $|\bar{B}_{10}|$ ) coefficients of the  $H_{10}$  wave on the normalized frequency for different values of the length of the waveguide twisted joint in the single-mode frequency range.

Next, we write integral equations (3) and (4) in  $4N$  points (where  $N$  is the approximation number), in which the elementary electric and magnetic dipoles oriented along the longitudinal coordinate are located. We find the numerical values of the surface integrals by substituting the field components into the indicated integral equations. As the result, we obtain the inhomogeneous system of  $4N$  linear algebraic equations. Solving this system, we find the unknown amplitude coefficients of the  $E$ - and  $H$ -type waves.

## 2. THE RESULTS OF THE CALCULATION OF THE TRANSMISSION CHARACTERISTICS OF A WAVEGUIDE TWISTED JOINT

Figure 5 shows the calculated dependences of the absolute values of the reflection and transmission coefficients of the fundamental wave  $H_{10}$  existing in the rectangular waveguide on normalized frequency  $ka$  for different values of length  $L$  of the waveguide twisted joint. The angle of the rotation of the waveguide twisted joint is  $\Gamma = 90^\circ$ . The results are obtained in the range of normalized frequencies  $3.14 \leq ka \leq 6.28$ , which corresponds to the single-mode regime of the guiding structure operation in the first approximation, when one  $H_{10}$  wave is taken into account in the regions of the regular waveguides and waveguide twisted joint.

In the figure, curves 1 and 2 are, respectively, the absolute values of the reflection and transmission coefficients of the  $H_{10}$  wave, when the length of the twisted joint is  $L = a$ , curves 3 and 4 correspond to  $L = 2a$ , curves 5 and 6 correspond to  $L = 3a$ , curves 7

and 8 correspond to  $L = 4a$ , and curves 9 and 10 correspond to  $L = 5a$ . It is seen from the figure that, when  $L \geq 2a$ , the value of the voltage standing wave ratio (VSWR) does not exceed 1.06 in the band of normalized frequencies  $3.6 \leq ka \leq 6.28$ . This fact indicates that the matching is good in the entire investigated frequency range.

We find the dependences of relative errors of the fulfillment of the energy conservation law (ECL) on the normalized frequency for different values of length  $L$  of the waveguide twisted joint for estimating the accuracy of the obtained results of the numerical realization of the developed algorithm. The relative error of the ECL fulfillment is determined as

$$\Delta = \left| \sum_{m,n} |\bar{R}_{mn}^{E,H}|^2 F^{E,H} + \sum_{m,n} |\bar{B}_{mn}^{E,H}|^2 K^{E,H} - 1 \right| \times 100\%,$$

$$F^E = \frac{\beta_{mn} \varepsilon}{\beta_{10} \mu} \left( m^2 + n^2 \frac{a^2}{b^2} \right), \quad K^E = \frac{\beta_{mn} \varepsilon}{\beta_{10} \mu} \left( m^2 \frac{ab}{ab} + n^2 \frac{a^2}{b^2} \right),$$

$$F^H = \frac{\beta_{mn}}{\beta_{10}} \left( m^2 + n^2 \frac{a^2}{b^2} \right), \quad K^H = \frac{\beta_{mn}}{\beta_{10}} \left( m^2 \frac{ab}{ab} + n^2 \frac{a^2}{b^2} \right),$$

where  $\beta_{10}$  is the longitudinal wave number of the wave  $H_{10}$ ;  $\beta_{mn}$  are the longitudinal wave numbers of the waves  $H_{mn}$  and  $E_{mn}$ ; and  $m$  and  $n$  are the wave indices corresponding to the wide and narrow walls of the guiding structure, respectively. The computational results for the frequency dependence of the relative error of the ECL fulfillment are shown in Fig. 6.

It is seen from the figure that the values of the relative error of the ECL fulfillment do not exceed 2.5% in

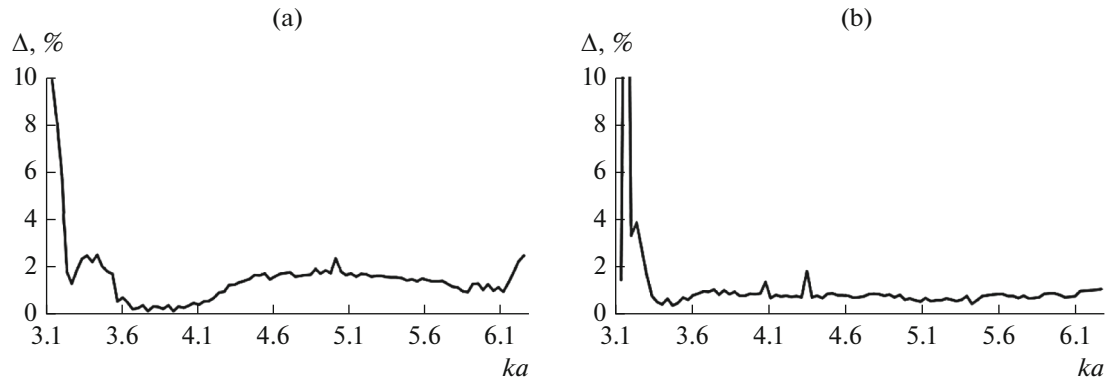


**Fig. 6.** Dependences of relative errors of the ECL fulfillment for the  $H_{10}$  wave in the single-mode range when length  $L$  of the waveguide twisted joint is (a)  $a$  and (b)  $3a$ .

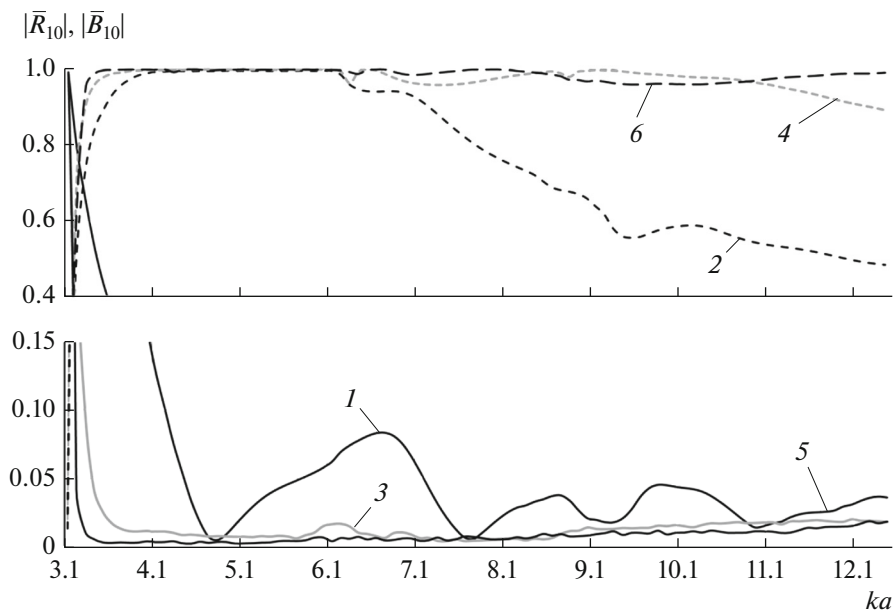


**Fig. 7.** Dependences of the absolute values of the (solid lines) reflection ( $|\bar{R}_{10}|$ ) and (dashed lines) transmission ( $|\bar{B}_{10}|$ ) coefficients of the  $H_{10}$  wave on the normalized frequency for different values of the length of the waveguide twisted joint in the multimode frequency range.

the entire investigated range of normalized frequencies with the exception of the region near the critical frequency of the fundamental wave  $H_{10}$ . We use four auxiliary magnetic-type sources (elementary magnetic dipoles) for the solution of the formulated diffraction problem. It is possible to state within the framework of the applied approximation that the chosen position of the auxiliary sources provides for the fulfillment of the condition that the indicated relative error does not exceed the ultimate permissible value equal to 5%.

In the context of this work, we calculate the transmission characteristics of the waveguide twisted joint in the wider range of normalized frequencies  $3.14 \leq ka \leq 12.56$ , which corresponds to its work in the multimode regime. Figure 7 shows the resulting calculated

dependences of the absolute values of the reflection and transmission coefficients for fundamental wave  $H_{10}$  of the rectangular waveguide on the normalized frequency for various values of the length of the waveguide twisted joint. The angle of the rotation of the waveguide twisted joint is  $\Gamma = 90^\circ$ . The results of calculation are obtained for the sixth approximation.

Figure 7 shows curves 1 and 2, which are the absolute values of the reflection and transmission coefficients, respectively, of wave  $H_{10}$  for the twisted joint length  $L = a$ ; curves 3 and 4 for  $L = 3a$ ; and curves 5 and 6 for  $L = 5a$ .

The curves of the absolute values of the reflection and transmission coefficients for the  $H_{10}$  wave have a



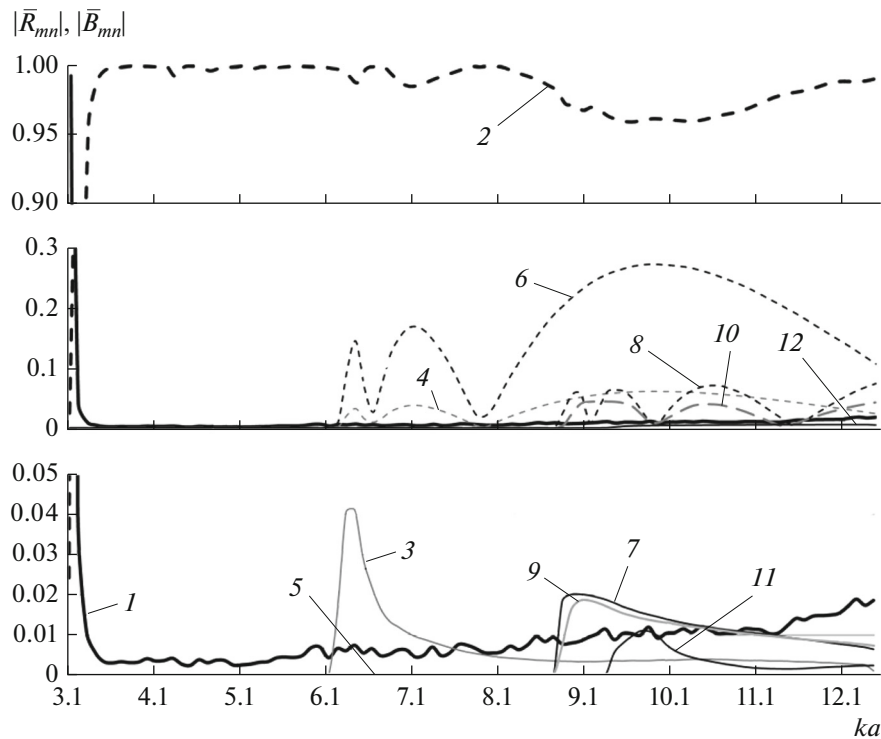


**Fig. 8.** Dependences of the absolute values of the (solid lines) reflection ( $|\bar{R}_{mn}|$ ) and (dashed lines) transmission ( $|\bar{B}_{mn}|$ ) coefficients of the  $H_{mn}$  and  $E_{mn}$  waves on the normalized frequency when the length of the waveguide twisted joint is  $L = 5a$  in the multimode frequency range.

complex frequency dependence in the frequency range corresponding to the multimode regime. This dependence is concerned with the characteristic properties of the energy exchange of the  $H_{10}$  wave with other waves propagating in the investigated guiding structure. Local maxima and minima in the frequency dependences of the transmission characteristics are observed near critical frequencies of higher-type waves. This effect can be explained by the appearance of the interaction between the wave indicated above and one of the mentioned waves.

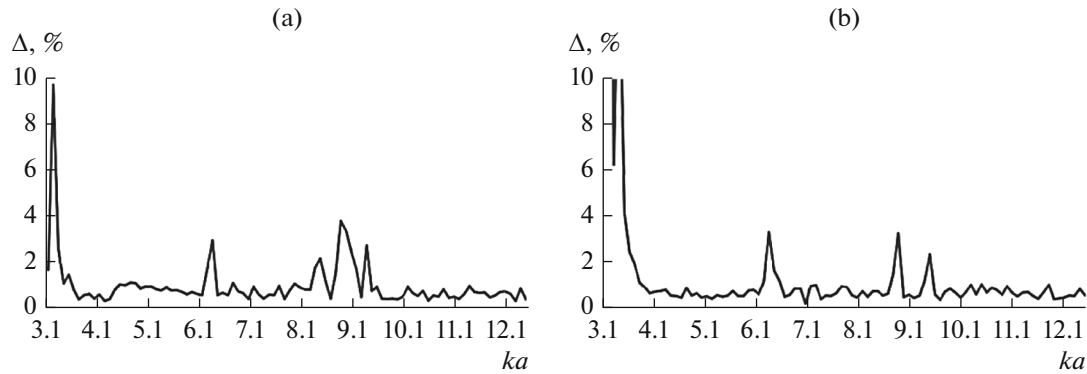
Figure 8 shows the frequency dependences of the absolute values of the reflection and transmission coefficients for waves  $H_{10}$ ,  $H_{20}$ ,  $H_{01}$ ,  $H_{21}$ ,  $E_{21}$ , and  $H_{30}$ , when the length of the waveguide twisted joint is  $L = 5a$ . The angle of the rotation of the waveguide twisted joint is  $\Gamma = 90^\circ$ .

It is seen from the figure that, in the frequency range corresponding to the multimode regime of the waveguide twisted joint operation, the diffraction of the  $H_{10}$  wave also results in the excitation and propagation in the regular waveguides waves  $H_{20}$ ,  $H_{01}$ ,  $H_{21}$ ,  $E_{21}$ , and  $H_{30}$ . Curves 1 and 2 in Fig. 8 are, respectively, the absolute values of the reflection and transmission coefficients for the wave  $H_{10}$ , curves 3 and 4 are the similar values for the wave  $H_{20}$ , curves 5 and 6 are the similar values for the wave  $H_{01}$ , curves 7 and 8 are

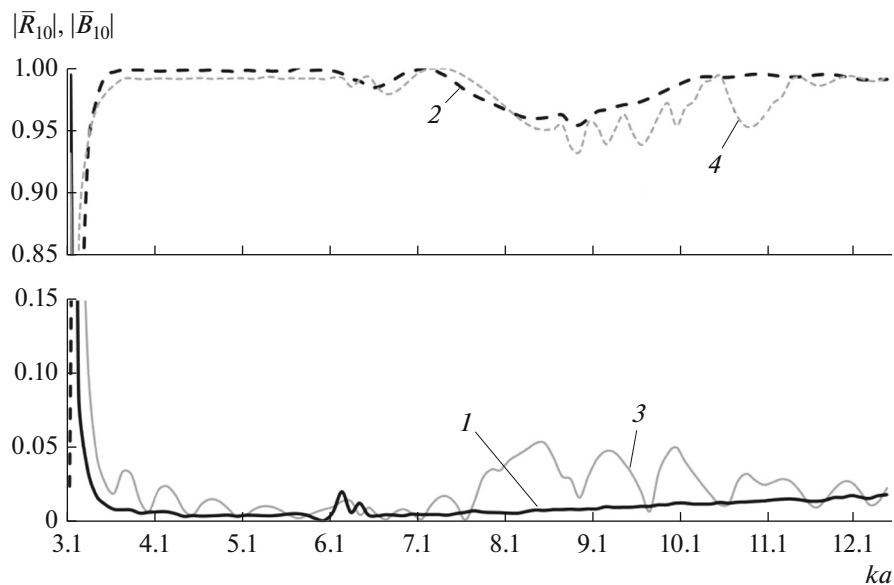
the similar values for the wave  $H_{21}$ , curves 9 and 10 are the similar values for the wave  $E_{21}$ , and curves 11 and 12 are the similar values for the wave  $H_{30}$ .

Figure 9 shows the dependences of the relative error of the ECL fulfillment on the normalized frequency in the multimode frequency range for different values of the waveguide twisted joint length. The indicated dependences are found for the purpose of estimating the accuracy of the calculation results obtained, when the developed algorithm is numerically realized. It is seen from the figure that, except for the region near the critical frequency of the  $H_{10}$  wave, the relative error of the ECL fulfillment in the entire considered range of the normalized frequencies does not exceed 4%. The peaks of the error of the ECL fulfillment are observed near the critical frequencies of the higher-type waves.

Proceeding from the presented above frequency dependences of the relative error of the ECL fulfillment, it is possible to conclude that the condition for keeping the indicated error from exceeding the threshold value (5%) is fulfilled. The problem is solved using the approximation  $N = 6$ , when five  $H$ -type waves and one  $E$ -type wave are taken into account. According to this, twenty longitudinally oriented magnetic dipoles and four electric dipoles are placed near the irregular region of the guiding structure. Their coordinates are



**Fig. 9.** Dependences of relative errors of the ECL fulfillment on the normalized frequency in the multimode range when length  $L$  of the waveguide twisted joint is (a)  $a$  and (b)  $3a$ .



**Fig. 10.** Dependences of the absolute values of the (solid lines) reflection ( $|\bar{R}_{10}|$ ) and (dashed lines) transmission ( $|\bar{B}_{10}|$ ) coefficients of the  $H_{10}$  wave on the normalized frequency for the length of the waveguide twisted joint  $L = 4a$  in the multimode frequency range.

determined using the recommendations given in works [12, 13].

The calculation results for the transmission characteristics of the waveguide twisted joint that are obtained with the help of the developed algorithm are compared with the results of calculation performed with the use of the computer-aided design (CAD) facility CST Microwave Studio. This is done in order to confirm the reliability of the obtained results. Figure 10 shows the calculation results for the transmission characteristics of the considered guiding structure, when the length of the waveguide twisted joint is  $L = 4a$ . These results are obtained using the proposed algorithm and CAD facility. The angle of the rotation of the waveguide twisted joint is  $\Gamma = 90^\circ$ .

Curves 1 and 2 in the figure are the absolute values of the reflection and transmission coefficients, respectively, that are obtained with the help of the developed algorithm, and curves 3 and 4 are obtained with the help of the CAD facility. Comparing the transmission characteristics, we can conclude that the results coincide qualitatively and quantitatively. The deviation of the calculation results obtained with the help of the CAD facility from the results obtained with the help of the developed algorithm does not exceed 3.5%. This fact confirms the correctness of the algorithm in the normalized frequency range corresponding to the multimode regime of the waveguide twisted joint work, when a finite set of higher-type waves is taken into account.

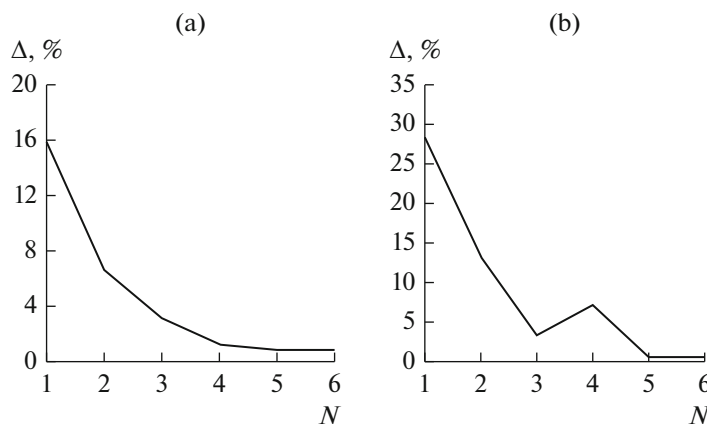


**Fig. 11.** Dependences of the relative error of the ECL fulfillment on the number of the approximation used for the solution of the problem for the waveguide twisted joint having the length  $L = 3a$  when  $ka$  is equal to (a) 7.46 and (b) 11.38.

The convergence of the solutions to the formulated diffraction problem is investigated in order to estimate the calculation method suggested in this work, the algorithm created on the basis of this method, and the validity of the obtained results. The results of the investigation are shown in Fig. 11. It is seen from the figure that relative error  $\Delta$  of the ECL fulfillment decreases and converges to zero, when the approximation number grows. In this case, the difference between the numerical values of the transmission characteristics in the fifth and sixth approximations does not exceed 0.2%. When the approximation number continues to grow, the numerical absolute values of the reflection and transmission coefficients insignificantly change and simultaneously considerable increases the SLAEs order. The performed investigation allows us to choose the working approximation  $N = 6$  for calculating the transmission characteristics of the waveguide twisted joint having a rectangular cross-section.

## CONCLUSIONS

The numerical-analytical method is proposed for the calculation of the transmission characteristics of the longitudinally–azimuthally irregular guiding structure in the form of a waveguide twisted joint having a rectangular cross-section. The presented algorithm is based on the method of integral equations [1–3, 8]. Each section of the irregular region in the considered guiding structure is matched with a comparison regular waveguide in order to write the field components on the surface of the irregular waveguide and find the values of the surface integrals entering the initial integral equations. The desired field is sought in the form of the superposition of the eigenmode fields of the corresponding comparison waveguides. Matching of the fields on the boundaries of the indicated decomposition sections of the irregular region is indirectly realized using integral equations (3) and (4).

The frequency dependences of the absolute values of the reflection and transmission coefficients for fundamental wave  $H_{10}$  of waveguide twisted joints of various lengths in single-mode and multimode regimes are found with the use of the developed algorithm. The transmission characteristics of higher-type waves are calculated and their effect on the reflection and transmission coefficients of fundamental wave  $H_{10}$  is investigated. The accuracy and correctness of the calculation results are confirmed by the dependences of the relative error of the ECL fulfillment on the normalized frequency and comparison with the results obtained with the help of CAD facilities. The validity of the application of the integral equation method and the numerical–analytical algorithm based on it is substantiated by the investigation of the convergence of the calculation results depending on the number of the approximation, in which the diffraction problem is solved. One of the main advantages of the proposed method is the reliability of the obtained results, which is well controlled. The nonstandard procedure of deriving the integral equations and the sufficient generality of application to the solution of inner boundary value diffraction problems are typical of the method.

## REFERENCES

1. S. B. Raevskii, *Fiz. Voln. Prots. i Radiotekh. Sist.* **12** (3), 34 (2009).
2. Yu. A. Ilarionov, A. S. Raevskii, S. B. Raevskii, and A. Yu. Sedakov, *Microwave Ovens and KVCh Devices of Ranges. Methods of Calculation. Algorithms. Manufacturing Techniques* (Radiotekhnika, Moscow, 2013) [in Russian].
3. Yu. G. Belov and S. B. Raevskii, *Izv. Vyssh. Uchebn. Zaved. Radiofiz.* **18**, 1523 (1975).
4. A. A. Metrikin, *Antennas and Wave Guides of RRL* (Svyaz', Moscow, 1977) [in Russian].

5. B. Z. Katsenelenbaum, *Theory of Waveguides with Slowly Varying Parameters* (Akad. Nauk SSSR, Moscow, 1961) [in Russian].
6. V. V. Shevchenko, *Continuous Transitions in Open Waveguides* (Nauka, Moscow, 1969; Golem, Boulder, Colo., 1971).
7. V. K. Maistrenko, A. A. Radionov, and S. B. Raevskii, *Elektrodin. i Tekh. SVCh&KVCh*, No. 4, 87 (1994).
8. Yu. A. Ilarionov, S. B. Raevskii, and V. Ya. Smorgonskii, *Calculation of Corrugated and Partly Filled Waveguide*, Ed. by V. Ya. Smorgonskii (Sovetskoe Radio, Moscow, 1980) [in Russian].
9. G. T. Markov, B. M. Petrov, and G. P. Grudinskaya, *Electromagnetics and Propagation of Radio Waves. Manual for Higher Education Institutions* (Sovetskoe Radio, Moscow, 1979) [in Russian].
10. I. N. Bronshtein and K. A. Semendyaev, *Handbook on Mathematics for Engineers and Students of High-Education Technical Institutes* (Nauka, Moscow, 1986) [in Russian].
11. G. A. Korn and T. M. Korn, *Mathematical Handbook for Scientists and Engineers* (McGraw-Hill, New York, 1968; Nauka, Moscow, 1973).
12. I. N. Danilov, V. K. Maistrenko, and C. E. Piliposyan, *Tr. NGTU im. R. E. Alekseeva*, No. 1 (80), 120 (2010).
13. S. M. Garanin, N. A. Novoselova, and S. B. Raevskii, *Antenny*, No. 11, 62 (2016).

Translated by I. Efimova